A Better Synthesis of Biruthenocene and Molecular Structures of $[Ru^{II}Cp(C_5H_4C_5H_4)CpRu^{IV}NCC_2H_5](BF_4)(B_2F_7)CH_3NO_2$, $[Ru^{II}Cp(2,2'\text{-bipyridine})(p\text{-benzoquinone})]BF_4$ and Related Salts

Masanobu Watanabe,* Masaru Sato, Akira Nagasawa,† Masahiro Kai,†† Izumi Motoyama,††† and Toshio Takayama†††

Chemical Analysis Center, Saitama University, Urawa, Saitama 338-8570

†Department of Chemistry, Faculty of Science, Saitama University, Urawa, Saitama 338-8570

††Faculty of Engineering, Tokyo Institute of Polytechnics, Atsugi, Kanagawa 243-0297

†††Department of Applied Chemistry, Faculty of Engineering, Kanagawa University, Rokkakubashi, Yokohama 221-8686

(Received October 7, 1998)

An interesting dimerization occurred during the oxidation of ruthenocene with an excess of *p*-benzoquinone containing $BF_3{\cdot}Et_2O$ (abbreviated *p*-Bq/BF_3) in a mixed solution of benzene and hexane, which gave biruthenocenium$(BF_4)_2$ (**A**) in 89% yield. Reduction of **A** with $TiCl_3$ gave biruthenocene in a good yield (68% from ruthenocene), which is the most elegant preparation of biruthenocene. Recrystallization of **A** from CH_3NO_2 containing C_2H_5CN gave a mixed-valence salt **3** formulated as $[Ru^{II}Cp(C_5H_4C_5H_4)CpRu^{IV}C_2H_5CN](BF_4)(B_2F_7)CH_3NO_2$ in which C_2H_5CN coordinated to the Ru^{IV} center. The crystal of **3** was found to be monoclinic, space group $P2_1/a$, a = 9.8930(8), b = 15.445(3), c = 19.728(3) Å, β = 92.57(1)°, V = 3011.3(1) Å^3, Z = 4, and the final R = 0.075 and R_w = 0.093. Recrystallization of **A** from CH_3NO_2 containing 2,2′-bipyridine and *p*-benzoquinone gave a yellow planar salt **4** formulated as $[Ru^{II}Cp(2,2'\text{-bipyridine})(p\text{-benzoquinone})]BF_4$ in which the olefin moiety of *p*-benzoquinone coordinated to the Ru^{IV} center in η^2-form. Salt **4** was also synthesized by the reaction of bromoruthenocenium (BF_4) with *p*-benzoquinone and 2,2′-bipyridine in CH_3NO_2. The crystal of **4** was found to be monoclinic, space group $P2_1$, a = 8.516(3), b = 9.934(4), c = 11.995(4) Å, β = 103.78(1)°, V = 985.6(6) Å^3, Z = 2, and the final R = 0.040 and R_w = 0.050. The same *p*-Bq/BF_3 oxidation of osmocene gave an orange red salt **5** formulated as $[Cp_2Os^{IV}FBF_3]BF_4$ in which one of the F^- atom of the BF_4^- ion coordinated to the Os^{IV} center. The crystal of **5** was found to be monoclinic, space group $P2_1/c$, a = 8.065(1), b = 12.048(1), c = 16.730(2) Å, β = 94.497(8)°, V = 1620.6(3) Å^3, Z = 4, and the final R = 0.055 and R_w = 0.070.

Recently, we have reported the structures of the mixed valence biruthenocenium salts ($Ru^{II}Ru^{IV}$) formulated as $[Ru^{II}Cp(C_5H_4C_5H_4)CpRu^{IV}L](BF_4)_2CH_3NO_2$ with a Ru^{IV}–L bond (L = acetonitrile (**1**), pyradine (**2**)) which are prepared by the oxidation of biruthenocene with *p*-Bq/BF_3.[1] To prepare analogous mononuclear ruthenocenium salts formulated as $[Cp_2Ru^{IV}L](BF_4)_2$, the similar *p*-Bq/BF_3 oxidation of ruthenocene was done. Contrary to our expectation, the main oxidation product **A** is not a mononuclear ruthenocenium cation but biruthenocenium dication. That is, unexpected dimerization occurred during the oxidation of ruthenocene with *p*-Bq/BF_3 as in the case of the reported air oxidation of ruthenocene in sulfuric acid.[2] The reduction of **A** with $TiCl_3$ gives neutral biruthenocene in a good yield (see Experimental section). The CH_3NO_2 solution of **A** containing CH_3CN, pyradine, and C_2H_5CN gives the mixed valence cations formulated as $[Ru^{II}Cp(C_5H_4C_5H_4)CpRu^{IV}L]$ (L = CH_3CN **1**, pyradine **2**, C_2H_5CN **3**), see Scheme 1. The CH_3NO_2 solution of **A** containing *p*-benzoquinone and 2,2′-bipyridine gives the π-complex cation formulated as $[CpRu^{II}$(2,2′-bipyridine)(*p*-benzoquinone)] (**4**). Unlike ruthenocene, the similar *p*-Bq/BF_3 oxidation of osmocene gives a mononuclear osmocenium salt **5**. These crystal structures of **3**, **4**, and **5** and their NMR spectral features are discussed here.

Experimental

Syntheses. The salts **1** and **2** were prepared by recrystallization of biruthenocenium$(BF_4)_2$ from CH_3NO_2 containing CH_3CN and pyradine by a method similar to that reported previously.[1]

Biruthenocenium$(BF_4)_2$ (A) and Biruthenocene. To a benzene solution (100 ml) of ruthenocene (RcH; 100 mg, 0.43 mmol) and *p*-benzoquinone (108 mg, 1.0 mmol) was added slowly a benzene–hexane solution (50 ml) of $BF_3{\cdot}Et_2O$ (0.06 ml, 2.0 mmol). After this was stirred for 30 min, the resulting dark-brown crude precipitates, which contained hydroquinone, were filtered. To remove the hydroquinone, the precipitates were washed with dry tetrahydrofuran and were recrystallized from a mixed solution of nitromethane and ether to give biruthenocenium$(BF_4)_2$ (**A**) as orange-yellow precipitates (121 mg, 0.191 mmol, 89% yield). IR (KBr) ν_{BF} 1100—1000 cm^{-1}. ^{1}H NMR (CD_3NO_2, 400 MHz) δ = 6.82 (t, 4H), 5.79 (s, 10H), 4.96 (t, 4H). ^{13}C NMR(CD_3NO_2, 100 MHz) δ = 95.7 (C_5H_4), 89.7 (C_5H_5), 87.0 (C_5H_4), 74.8 (*ipso*-C_5H_4). Found: C,

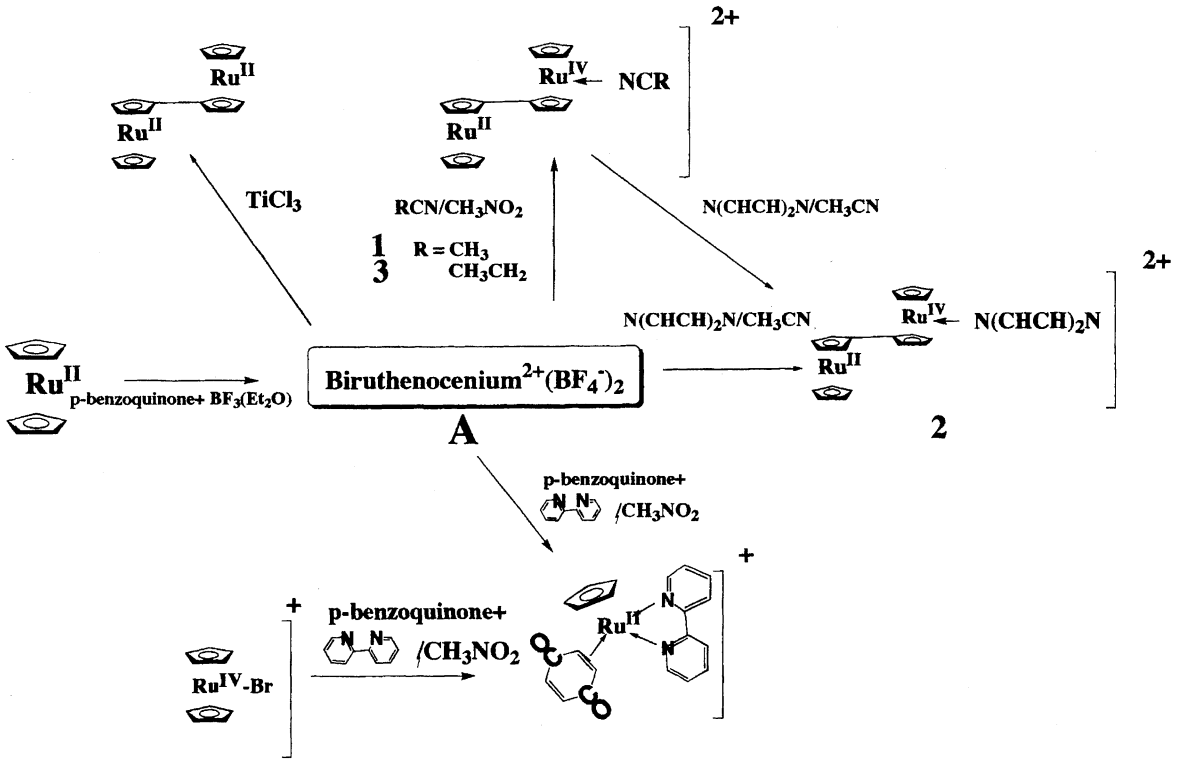

Scheme 1.

37.95; H, 2.90%. Calcd for $C_{20}H_{18}B_2F_8Ru_2$: C, 37.88; H, 2.86%.

A (100 mg, 0.158 mmol) was dissolved in CH_3CN (10 ml), and then was poured into water containing a large excess of $TiCl_3$, losing its color. The organic phase was extracted with benzene and the extract was washed with water, dried, and evaporated. The residue was purified by column chromatography by the same procedure reported in the preparation of biruthenocene from ruthenocene in concentrated H_2SO_4.[2] The light yellow precipitates (55 mg, 0.119 mmol, 76% yield) were obtained. The ^{1}H NMR, IR, and elemental analysis data correspond well those reported for biruthenocene.

$[Ru^{II}Cp(C_5H_4C_5H_4)CpRu^{IV}(NCC_2H_5)](BF_4)(B_2F_7)CH_3NO_2$ (3). **A** (100 mg, 0.158 mmol) was dissolved in CH_3NO_2 (10 ml) containing C_2H_5CN (0.04 ml), giving a deep-red solution. To prepare well formed single crystals, BF_3·Et_2O (0.03 ml) and diethyl ether were added to the solution. Deep-red plates (52 mg, 0.064 mmol; yield 41%) were formed after keeping for several days at about 260 K. IR (KBr) ν_{NO} (nitromethane) 1555 cm^{-1}, ν_{BF} 1100—1000 cm^{-1}. ^{1}H NMR (CD_3COCD_3) δ = 6.65 (t, 2H), 6.07 (s, 5H), 6.01 (t, 2H), 5.86 (t, 2H), 5.73 (t, 2H), 5.01 (s, 5H), 4.42 (s, 3H, CH_3NO_2), 2.93 (q, 2H, C_2H_5CN), 1.14 (t, 3H, C_2H_5CN). Found: C, 35.52; H, 3.28; N 3.52%. Calcd for $C_{24}H_{26}B_3F_{11}N_2O_2Ru_2$: C, 35.24; H, 3.20; N, 3.42%.

$[Ru^{II}Cp(C_5H_4N)_2(p\text{-}C_6H_4O_2)](BF_4)_2$ (4). The salt **4** was prepared by the following two methods.

(1) **A** (100 mg, 0.158 mmol) was dissolved in CH_3NO_2 (10 ml) containing 2,2′-bipyridine (25.0 mg, 0.16 mmol) and *p*-benzoquinone (17.0 mg, 0.16 mg) at room temperature. The solution was stirred for about 3 h. Single crystals suitable for X-ray studies were obtained by diffusion of diethyl ether into the solution at about 260 K for several days, well-formed yellow plane crystals **4** (12 mg; 0.023 mmol; yield 15%) were obtained.

(2) Bromoruthenocenium(BF_4) ([$RuCp_2Br$]BF_4) (100 mg, 0.25 mmol) were dissolved in CH_3NO_2 (10 ml) containing 2,2′-bipyridine (39.0 mg, 0.25 mmol) and *p*-benzoquinone (27.0 mg, 0.25 mmol). The solution was stirred for 2 h at about 320 K. Salt **4** was purified by column chromatography on silica gel. Salt **4** was eluted by CH_3NO_2 as an orange-yellow band, which was recrystallized from a mixed solution of CH_3NO_2 and $C_2H_5OC_2H_5$ as yellow precipitates (52 mg, 0.010 mmol, 40% yield). IR (KBr) ν_{CO} (*p*-benzoquinone) 1644, 1631 cm^{-1}, ν_{BF}(BF_4) 1100—1000 cm^{-1}. ^{1}H NMR(CD_3CN) δ = 8.71 (d, 2H), 8.27 (d, 2H), 8.08 (t, 2H), 7.58 (t, 2H), 5.35 (s, 5H, C_5H_5), 5.25 (s, 2H, $C_6H_4O_2$), 5.20 (b, 2H, $C_6H_4O_2$). Found: C, 48.49; H, 3.21; N, 5.36%. Calcd for $C_{21}H_{17}BF_4N_2O_2Ru$: C, 48.76; H, 3.31; N, 5.42%.

$[Cp_2Os^{IV}FBF_3](BF_4)CH_3NO_2$ (5). To a solution of osmocene (50 mg; 0.16 mmol) containing *p*-benzoquinone (54.1 mg; 0.50 mmol) in benzene (50 ml), a mixed solution of benzene (2 ml) and hexane (10 ml) containing BF_3·Et_2O (0.05 ml) was added. The solution was stirred for 2 h, and then dark-yellow precipitates were formed. The precipitates were filtered off and dissolved in CH_3NO_2 giving a red solution. To the solution, diethylether was added, and well formed single crystals **5** were obtained after keeping for several days at about 260 K (28 mg, 0.050 mmol, 31%). IR (KBr) ν_{BF} 1000—1100 cm^{-1}. ^{1}H NMR (CD_3NO_2) δ = 6.09 (s, 10H). Found: C, 23.53; H, 2.31; N; 2.42%. Calcd for $C_{11}H_{13}B_2F_8NO_2Os$: C, 23.80; H, 2.36; N, 2.52%.

NMR, Cyclic Voltammetry, and X-Ray Analysis. The ^{1}H NMR spectra (400.134 MHz) were recorded at 298 K on a Bruker AM400 spectrometer and referred to TMS as an internal standard. IR spectra were recorded on Perkin–Elimer System 2000 spectrometer. Cyclic voltammetry was done using ALS CH instruments in 10^{-1} M *n*-Bu_4NClO_4 solution in CH_2Cl_2 (1 M = 1

mol dm^{-3}). The cell was fitted with a glassy carbon (GC) working electrode, platinum wire counter electrode, and Ag–Ag$^+$ pseudo-reference electrode, and the scan rate was 0.1 V s^{-1}. All potentials were referred to ferrocene-ferrocenium, which were obtained by subsequent measurement under the same conditions.

The X-ray diffraction measurements were done on a MAC Science Rapid Diffraction Image Processor (DIP 3000) with graphite-monochromatized Mo $K\alpha$ radiation and a 18-kW rotation-anode generator. Refections were collected using 30 continuous Weissenberg photographs with a ϕ range of 6° (total range, 0—180°). The intensity data were corrected for the standard Lorentz and polarization effects. The structure was solved with the Dirdif–Patty method in the CRYSTAN-GM (software-pack for structure analysis) and refined finally by the full-matrix least squares procedure. An anisotropic refinement for non-hydrogen atoms was done. All the hydrogen atoms, partially located from difference Fourier maps, were isotropically refined. The crystallographic data and some of the experimental conditions for the X-ray structure analysis of **3**, **4**, and **5** are listed in Table 1. Tables of the atomic coordinates thermal parameters, bond distances, and $F_o - F_c$ data for **3**, **4**, and **5** are deposited as Document No. 72012 at the Office of the Editor of Bull. Chem. Soc. Jpn.

Results and Discussion

Preparation of Biruthenocene and Structures of 3 and 4. When the benzene–hexane solution containing $BF_3 \cdot Et_2O$ was added to a solution of ruthenocene and *p*-benzoquinone in benzene, dark blown precipitates were obtained immediately. The precipitates were well soluble in CH_3CN, giving deep red solutions. The color was not that of the typical mononuclear ruthenocenium cations (yellow-green) but that of the mixed-valence ($Ru^{II}Ru^{IV}$) biruthenocenium cations formulated as $[Ru^{II}Cp(C_5H_4C_5H_4)CpRu^{IV}X]$ (X = Cl, Br, I).[2] In ^{1}H NMR spectrum of **A** in CD_3CN, six sharp signals ascribed to the Cp- and C_5H_4-ring protons were found (δ = 6.24 (t, 2H), 5.72 (t, 2H), 5.71 (s, 5H) ascribed to the $[Ru^{IV}Cp(C_5H_4)NCCH_3]^{2+}$ moiety and 5.52 (t, 2H), 5.32 (t, 2H), 4.90 (s, 5H) to the $Ru^{II}Cp(C_5H_4)$ moiety). All the δ values correspond well to the reported cation, $[Ru^{II}Cp(C_5H_4C_5H_4)CpRu^{IV}NCCH_3]$ [**A·CH$_3$CN**], which was prepared by a similar oxidation of biruthenocene with *p*-Bq/BF_3;[1] i.e., the dimerization of ruthenocene must have occurred during the *p*-Bq/BF_3 oxidation. The recrystallization of **A** from CH_3NO_2 containing C_2H_5CN and BF_3 gave deep red planar crystals **3**. To verify this astonishing result, X-ray diffraction of **3** was done.

Salt **3** crystallized in the monoclinic space group $P2_1/a$. Select interatomic distances and angles are shown in Table 2 and ORTEP drawings of **3** are shown in Figs. 1a and 1b, along with the atom numbering system.

The X-ray diffraction study showed that the structure of **3** is the mixed valence biruthenocenium cation formulated as $[Ru^{II}Cp(C_5H_4C_5H_4)CpRu^{IV}NCC_2H_5]^{2+}$, that is, the dimerization of ruthenocene by the oxidation of *p*-Bq/BF_3 is verified. We have reported a similar dimerization of ruthenocene from air oxidation in sulfuric acid.[2] Thus, it can be concluded that some oxidations of ruthenocene give dimerization products. Considering these facts, a possible mechanism of the formation of **A** may be explained as follows (see Scheme 2).

Ruthenocene is first oxidized giving an unstable ruthenocenium ion $[Cp_2Ru^{III}]^+$, which abstracts intermolecularly a hydrogen atom from ruthenocene to give a relatively stable protonated ion, $[Cp_2RuH]^+$, and a ruthenocenyl radical $[CpRuC_5H_4\cdot]$. Two of the latter are coupled with each other to give biruthenocene. Continuously, biruthenocene is oxidized by *p*-Bq/BF_3 giving a dicationic biruthenocenium^{2+} ion. The driving force of the coupling must be ascribed to the unstable ruthenocenium ion $(Cp_2Ru^{III})^+$ (the cation was

Table 1. Crystal and Intensity Collection Data for **3**, **4**, and **5**

	3	**4**	**5**
Formula	$C_{24}H_{26}B_3F_{11}N_2O_2Ru_2$	$C_{21}H_{17}BF_4N_2O_2Ru$	$C_{11}H_{13}B_2F_8NO_2Os$
Formula weight	818.03	517.25	555.03
Size of crys./mm	0.25 × 0.20 × 0.08	0.12 × 0.15 × 0.05	0.23 × 0.25 × 0.15
Space group	$P2_1/a$	$P2_1$	$P2_1/c$
a/Å	9.8930(8)	8.516(3)	8.065(1)
b/Å	15.445(3)	9.934(4)	12.048(1)
c/Å	19.728(3)	11.995(4)	16.730(2)
β/°	92.57(1)	103.78(1)	94.497(8)
V/Å^3	3011.3(1)	985.6(6)	1620.6(3)
Z	4	2	4
T/K	298	298	298
λ/Å	0.71073	0.71073	0.71073
D_x	1.876	1.743	2.275
No. of reflns meased	7814	2187	4969
No. of reflns unique	6592	1844	4317
No. of reflns.	3706 ($I > 2\sigma(I)$)	1588 ($I > 3\sigma(I)$)	3171 ($I > 2\sigma(I)$)
R[a]	0.075	0.040	0.055
R_w[b]	0.093	0.050	0.070
$(\Delta/\sigma)_{max}$	0.75	0.71	0.499
$\Delta\rho_{min}$, $\Delta\rho_{max}$/e Å^{-3}	−1.08, 1.26	−1.55, 2.15	−1.80, 1.03

a) $R = \sum||F_o| - |F_c||/\sum|F_o|$. b) $R_w = [\sum w(|F_o| - |F_c|)^2/\sum w|F_o|^2]^{1/2}$.

Table 2. Selected Bond Distances and Angles for **3**

Atom 1 Atom 2	Dist/Å	Atom 1 Atom 2	Dist/Å
Ru(1)–C(1)	2.21 (3)	Ru(2)–C(11)	2.44 (1)
Ru(1)–C(2)	2.15 (2)	Ru(2)–C(12)	2.25 (1)
Ru(1)–C(3)	2.17 (2)	Ru(2)–C(13)	2.16 (1)
Ru(1)–C(4)	2.16 (2)	Ru(2)–C(14)	2.18 (2)
Ru(1)–C(5)	2.11 (3)	Ru(2)–C(15)	2.26 (1)
Ru(1)–C(6)	2.15 (1)	Ru(2)–C(16)	2.20 (1)
Ru(1)–C(7)	2.16 (1)	Ru(2)–C(17)	2.20 (1)
Ru(1)–C(8)	2.21 (2)	Ru(2)–C(18)	2.23 (1)
Ru(1)–C(9)	2.23 (2)	Ru(2)–C(19)	2.17 (1)
Ru(1)–C(10)	2.17 (1)	Ru(2)–C(20)	2.22 (1)
Ru(2)–N(1)	2.07 (1)	N(1)–C(21)	1.13 (2)
C(1)–C(2)	1.30 (3)	C(1)–C(5)	1.38 (4)
C(2)–C(3)	1.32 (3)	C(3)–C(4)	1.39 (3)
C(4)–C(5)	1.49 (4)	C(6)–C(7)	1.44 (2)
C(6)–C(10)	1.41 (2)	C(7)–C(8)	1.43 (2)
C(8)–C(9)	1.42 (2)	C(9)–C(10)	1.41 (2)
C(6)–C(11)	1.46 (1)	C(11)–C(12)	1.42 (2)
C(11)–C(15)	1.41 (1)	C(12)–C(13)	1.41 (2)
C(13)–C(14)	1.42 (3)	C(14)–C(15)	1.40 (2)
C(16)–C(17)	1.42 (3)	C(16)–C(20)	1.41 (3)
C(17)–C(18)	1.36 (3)	C(18)–C(19)	1.39 (3)
C(19)–C(20)	1.43 (3)	C(21)–C(22)	1.44 (3)
C(22)–C(23)	1.43 (3)		
B(1)–F(1)	1.36 (3)	B(1)–F(2)	1.32 (3)
B(1)–F(3)	1.30 (3)	B(1)–F(4)	1.35 (3)
B(2)–F(5)	1.29 (3)	B(2)–F(6)	1.26 (3)
B(2)–F(7)	1.39 (3)	B(2)–F(8)	1.52 (3)
B(3)–F(8)	1.51 (2)	B(3)–F(9)	1.33 (3)
B(3)–F(10)	1.32 (3)	B(3)–F(11)	1.40 (3)
Bond angles			
Ru(2)–N(1)–C(21)	175(1)	N(1)–C(21)–C(22)	178(2)
C(21)–C(22)–C(23)	117(2)	B(2)–F(8)–B(3)	129(1)
O(1)–N(2)–O(2)	125(2)	O(2)–N(2)–C(24)	118(2)
O(1)–N(2)–C(24)	117(2)		

Dihedral angle plane	C(1–5)	C(6–10)	C(11–15)	C(16–20)
C(1–5)	—	3.75	18.40	58.86
C(6–10)	—	—	21.52	62.12
C(11–15)	—	—	—	40.61

only identified from the study of a cyclic voltammogram in an extremely weak coordinating supporting electrolyte and solvent (CH_2Cl_2)[3]). The $TiCl_3$-reduction of **A** gave neutral biruthenocene in a good yield (68% from ruthenocene). This is the most elegant preparation of biruthenocene, to our knowledge.

The molecular structure of **3** is fundamentally similar to that of **1**. The Ru(1)···Ru(2) distance (5.320(1) Å), the mean Ru–C_{ring} distance (2.17(3) Å for Ru^{II}, 2.28(9) Å for Ru^{IV}), the Ru–Cp distance (1.815(1) Å for Ru^{II}, 1.88(2) Å for Ru^{IV}) are closer to those of **1**.[1]) The coordination mode of C_2H_5CN to the Ru^{IV} (the Ru^{IV}–N distance, 2.07(1) Å, the Ru(2)–N(1)–C(21) angle 175(1)°, the C≡N distance, 1.13(2) Å) is nearly the same with those of CH_3CN in **1** (the Ru^{IV}–N distance, 2.04(2) Å, the Ru(2)–N(1)–C(21) angle, 174(1)°, the C≡N distance, 1.13(2) Å).[1]) The most interesting difference of **3** from **1** is found in the direction of the Ru–N(1) bond toward the $C_5H_4C_5H_4$ plane (see Fig. 1b). The C_2H_5CN molecule in **3** is located just in the center of the fulvalene ligand (the torsion angle N(1)–Ru(2)–C(11)–C(6), about 1.6(9)°, see Fig. 1b), while the CH_3CN molecule in **1** is coordinated to the Ru^{IV} from the oblique direction of the plane (the torsion angle, 20°[1]). The latter mode must be caused by the steric hindrance between the coordinated CH_3CN and the BF_4^- from the crystal packing.[1]) For **3**, since the absence of such steric hindrance between the coordinated C_2H_5CN and the F atoms of the anions (BF_4^- and $B_2F_7^-$, the shortest intermolecular distance between the C atoms of C_2H_5CN and the F atoms of anions is 3.17 Å (F(10)–C(23)), which is larger than the sum (3.05 Å) of van der Waals radii of F and C[4]), the C_2H_5CN molecule is located just in the center of the fulvalene ligand.

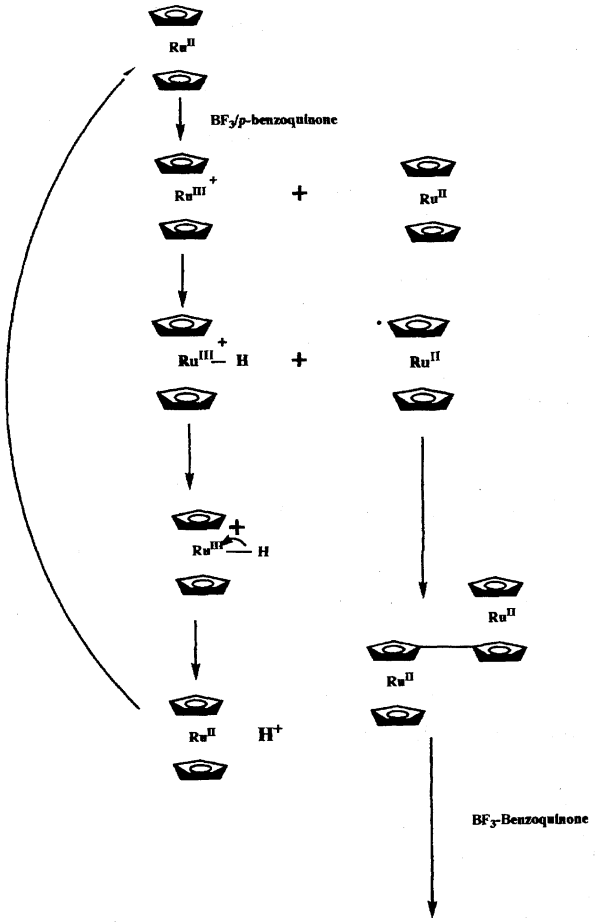

Scheme 2.

The tilt angle (40.61°) between the Cp and C_5H_4 planes in $CpC_5H_4Ru^{IV}$ moiety is considerably larger than the values of **1** (38.70°), $[C_5Me_4(CH_2)_3C_5Me_4M^{IV}NCCH_3]^{2+}$ (34.5° for M = Fe and 34.83° for Ru[5]), and $[RuCp(\eta^4\text{-}C_5H_3O\text{-}2\text{-}PPh_3)NCCH_3]^{2+}$ (35.5 (7)°[6]), while its value on the Ru^{II} side is 3.75°. The dihedral angle (21.52°) between the planes

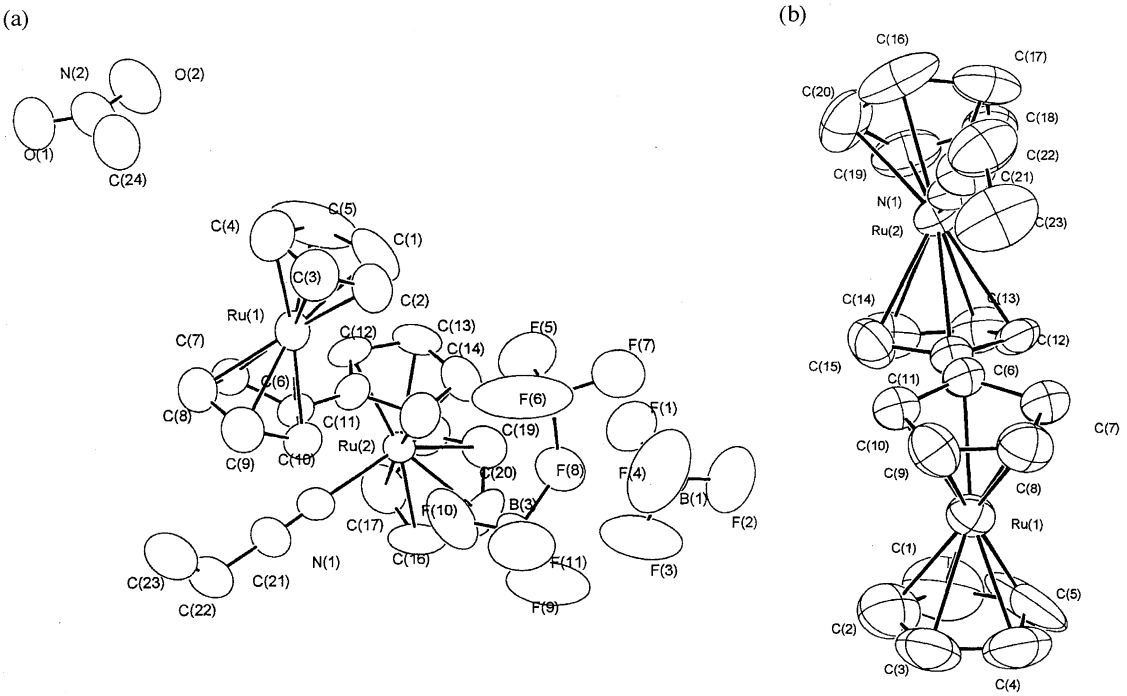

Fig. 1. (a) ORTEP drawing of **3** with the thermal ellipsoids at the 50% probability level. (b) ORTEP drawing of the dication $[Ru^{II}Cp(C_5H_4C_5H_4)CpRu^{IV}NCCH_3]^{2+}$ **3** with the numbering of the atoms.

C(6–10) and C(11–15) is also much larger than the value of **1** (17.04°). These phenomena may be caused by the van der Waals repulsion between the $C_5H_4C_5H_4$ ligand and coordination of more balkiness of C_2H_5CN than that of CH_3CN. The distance N(1)···C(6) (2.93(1) Å) and N(1)···C(11) (2.69(1) Å) are much smaller than the sum (3.20 Å) of the van der Waals radii of the N and C atom[4]) and then the C(6) and C(11) atoms are located far out of the plane (C(12)–C(13)–C(14)–C(15)), giving the much longer Ru(2)–C(11) distance (2.44(1) Å) compared with other values of Ru–C (2.258—2.167 Å).

The other remarkable feature in the crystal of **3** is the presence of the $B_2F_7^-$ anion, which was the first identified by X-ray diffraction, to our knowledge. The F atom of BF_4^- anion is coordinated to the B atom of the BF_3 molecule (a Lewis acid), giving the F–B–F bridged structure of $B_2F_7^-$ anion. The bridging bond angle, B(2)–F(8)–B(3), and mean bridging bond distance, B–F(8), of $B_2F_7^-$ anion were found to be 129(1)°, 1.51(1) Å, respectively. The latter is much larger than the mean value of the $B–F_{terminal}$ (1.33(5) Å) and mean B–F distance of the BF_4^- (1.33(2) Å) because of the ligation of the F(8) to the B(2) and B(3) atoms. In the ^{19}F NMR spectrum of **3**, done in CD_3CN at 298 K, two signals were found at $\delta = -146$ for the BF_4^- and $\delta = -147$ for the $B_2F_7^-$ ions. Only one F signal was observed for bridged $B_2F_7^-$ anion, suggesting the $F_{terminal}$ and F_{bridge} atoms of the $B_2F_7^-$ anion are equivalent in NMR time scale at room temperature, suggesting the presence of a fast dynamic motion ($F_3BF'BF_3 \leftrightarrows F_3BFBF_2F'$) in solution.

The ^1H NMR spectrum of **3** in CD_3COCD_3 was essentially similar to that of **1**. The δ values of Cp and $C_5H_4C_5H_4$ were very similar to those of **1**, see Experimental section. The coordinated C_2H_5CN molecule gave two signals (δ = 1.14 (3H, t) for $-CH_3$, 2.93 (2H, q) for $-CH_2-$). Compared with the values of free C_2H_5CN (δ = 1.22 (3H, t) for $-CH_3$, 2.42 (2H, q) for $-CH_2-$) under the same conditions, a significant large lower field shift ($\Delta\delta$ = 0.51 ppm) was observed for the methylene signal of the coordinated C_2H_5CN. This is somewhat smaller than the value of **1** (0.6 ppm) and $[OsCp_2NCCH_3]$ (0.9 ppm[7]), suggesting a weaker $Ru^{IV}–NCC_2H_5$ bond of **3** compared with the $Ru^{IV}–NCCH_3$ bond of **1**. Actually based on the result of the ^1H NMR spectrum of **3** in CD_3CN, the coordinated C_2H_5CN was easily replaced by CD_3CN immediately because of the stronger nucleophilicity of CH_3CN to the Ru^{IV} center compared with CH_3CH_2CN.

Recrystallization of **A** from CH_3NO_2 containing 2,2′-bipyridine and *p*-benzoquinone gave salt **4** as yellow planar precipitates. The NMR spectrum of **4** in CD_3CN was quite different from those of the mixed-valence $Ru^{II}Ru^{IV}$ salts **1**—**3**. In the spectrum of **4** no fulvalene signal was observed, suggesting that the loss of the fulvalene ligand occurred during the ligation of 2,2′-bipyridine. Similarly, **4** is also obtained by the reaction of bromoruthenocenium cation, $[Cp_2RuBr]^+$, with an equivalent amount of 2,2′-bipyridine and *p*-benzoquinone in CH_3NO_2.

The salt **4** crystallized in the monoclinic space group $P2_1$. The selected interatomic distance and angles for **4** are shown in Table 3 and the ORTEP drawing of the cations are shown in Fig. 2, along with the atomic numbering.

. The most interesting structural feature in the cation of **4** is coordination of 2,2′-bipyridine and *p*-benzoquinone to the Ru center, other than the Cp ligand. The $C_5H_4C_5H_4$

ligand of cation **A** is eliminated during the coordination of strongly nucleophilic and cheleting 2,2′-bipyridine to the Ru center. The mean Ru–Cp and Ru–C_{ring} distances are 1.843 and 2.19(5) Å, respectively. On the results of the elemental analysis and X-ray diffraction study, the formal oxidation state of the Ru atom is Ru^{II} and salt **4** is formulated as [Ru^{II}Cp-(2,2′-bipyridine)(*p*-benzoquinone)]BF_4. Reduction of the central Ru atom from Ru^{IV} to Ru^{II} may have occurred during of the elimination of the fulvalene ligand.

The distance between the Ru(1) and N(1) and N(2) in **4** are 2.11(2) and 2.08(1) Å, respectively, which are somewhat longer than the reported Ru^{II} analogous salts; [Ru(2,2′-bipyridine)$_3$] (2.056(2) Å), [Ru(2,2′-bipyrimidine)$_3$] (2.067(4) Å), and [Ru(2,2′-bipyrazine)$_3$] (2.05(1) Å) cations.[8] The N(1)–Ru–N(2) bond angle is 75.8(3)°, which is somewhat smaller than the values of [Ru(2,2′-bipyridine)$_3$] (78.7(1)°), [Ru(2,2′-bipyrimidine)$_3$] (78.3(3)°), and [Ru(2,2′-bipyrazine)$_3$] (78.6(4)°) cations.[8]

From these results, it was concluded that there is no significant difference in the coordination structure around the Ru^{II}–2,2′-bipyridine moiety, however, the most interesting feature in **4** is the coordination of *p*-benzoquinone in η^2-form. To the best of our knowledge, this is the first η^2-complex of *p*-benzoquinone, although many η^4-tetramethyl-1,4-benzoquinone complexes and related complexes have been reported.[9—12] The Ru–C(16) and Ru–C(17) distances are 2.21(1) and 2.22(1) Å, respectively, the values are comparable with the distance of the Ru–C_{ring}. The C(16)–C(17) distances of the coordinated double bond (1.44(1) Å) is much larger than the C(19)–C(20) distance (1.30(3) Å) of the other olefinic bond, because of the coordination to the Ru^{II}.

The dihedral angle between the plane C(16)–C(17)–Ru-(1) and the plane C(16–21) is 76.3°, supporting the η^2-coordination of the C(16)–C(17) double bond to the Ru^{II} atom. The plane of *p*-benzoquinone C(16–21) keeps good planarity and the dihedral angle between the plane of the cyclopentadienyl ligand C(1–5) and the plane C(16–21) is 74.3°. To reduce steric hindrance between the Cp ligand and 2,2′-bipyridine, *p*-benzoquinone is ligated to the Ru atom in the direction facing the 2,2′-bipyridine ligand (see Fig. 2).

In the ^{1}H NMR spectroscopy of **4** in CD_3CN, two broad signals at δ = 5.37 (s, 2H) and 5.04 (s, 2H) due to the olefinic proton of the coordinated *p*-benzoquinone are observed at 270 K. The δ values are shifted to a much higher field compared with that of free *p*-benzoquinone in CD_3CN (δ = 6.63). When the temperature is raised (305 K), the broad signals become sharp and approached each other (δ = 5.31 and 5.27), suggesting a certain dynamic motion between the free and the coordinated double bonds upon heating. On heating for 30 min, **4** was decomposed with the color of the solution changing from yellow to orange. The ^{1}H NMR spectrum of the solution at 305 K, the protons for the coordinated 2,2′-bipyridine at δ = 9.51 (d, 2H), 8.31 (d, 2H), 8.05 (t, 2H) and 7.54 (t, 2H) and that for the Cp-ring at δ = 4.47 (s, 5H) and that for the free *p*-benzoquinone at δ = 6.80 (s, 4H) were found. The observation may suggest clearly that the coordinated *p*-benzoquinone is substituted by CH_3CN.

Table 3. Selected Bond Distances and Angles for **4**

Atom 1 Atom 2	Dist/Å	Atom 1 Atom 2	Dist/Å
Ru(1)–C(1)	2.18 (1)	Ru(1)–C(2)	2.21 (2)
Ru(1)–C(3)	2.26 (2)	Ru(1)–C(4)	2.19 (2)
Ru(1)–C(5)	2.18 (2)	Ru(1)–C(16)	2.21 (1)
Ru(1)–C(17)	2.22 (1)	Ru(1)–N(1)	2.11 (2)
Ru(1)–N(2)	2.08 (1)		
C(1)–C(2)	1.46 (3)	C(1)–C(5)	1.36 (2)
C(2)–C(3)	1.42 (3)	C(3)–C(4)	1.39 (3)
C(4)–C(5)	1.43 (3)	C(6)–C(7)	1.41 (2)
C(6)–N(1)	1.36 (1)	C(7)–C(8)	1.35 (2)
C(8)–C(9)	1.37 (2)	C(9)–C(10)	1.38 (2)
C(10)–N(1)	1.35 (1)	C(11)–C(12)	1.36 (2)
C(11)–N(2)	1.37 (2)	C(12)–C(13)	1.37 (2)
C(13)–C(14)	1.39 (2)	C(14)–C(15)	1.37 (2)
C(16)–C(17)	1.44 (1)	C(16)–C(21)	1.45 (1)
C(17)–C(18)	1.46 (1)	C(18)–C(19)	1.48 (1)
C(19)–C(20)	1.30 (3)	C(20)–C(21)	1.52 (2)
C(18)–O(1)	1.25 (1)	C(21)–O(2)	1.22 (1)
B(1)–F(1)	1.38 (3)	B(1)–F(2)	1.38 (3)
B(1)–F(3)	1.31 (2)	B(1)–F(4)	1.24 (3)

Bond angles

C(16)–Ru(1)–C(17)	37.6(3)	N(1)–Ru(1)–N(2)	75.8(3)
Ru(1)–C(16)–C(17)	71.5(6)	Ru(1)–C(17)–C(16)	70.9(6)
C(16)–C(17)–C(18)	121.5(7)	C(17)–C(16)–C(21)	120.2(7)

Dihedral angle

plane	C(1–5)	N(1)–C(6–15)–N(2)	C(16–21)
C(1–5)	—	136.5	74.3
N(1)–C(6–15)–N(2)	—	—	30.4

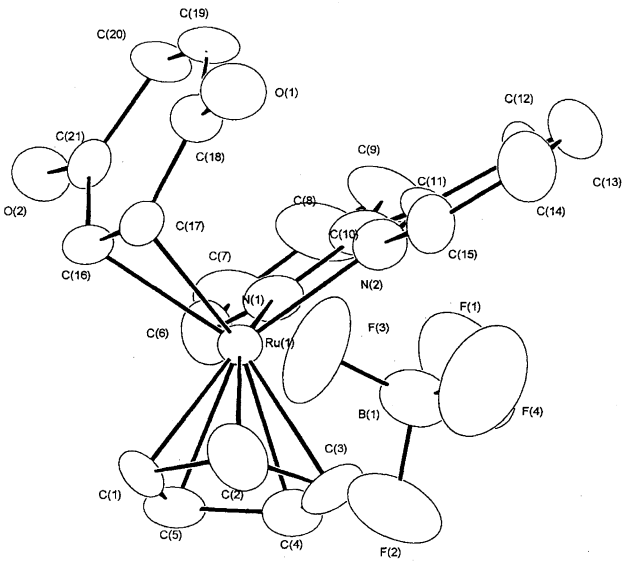

Fig. 2. ORTEP drawing of **4** with the thermal ellipsoids at the 50% probability level.

Structure of 5. For a long time no preparation of biosmocene have been reported (biosmocene was not prepared by air oxidation of osmocene in sulfuric acid under similar conditions to those for biruthenocene,[2] but this study suggests the possibility of preparation of biosmocene by the *p*-

Bq/BF_3 oxidation of osmocene in a similar manner. The *p*-Bq/BF_3 oxidation of osmocene in hexane–benzene solution gave dark yellow precipitates. The recrystallization of the resulting oxidation product from CH_3NO_2 gave orange-red micro crystals **5**. Salt **5** crystallized in the monoclinic space group $P2_1/c$. The selected interatomic distances and angles for **5** are shown in Table 4 and the ORTEP drawing of the cations is shown in Fig. 3 along with the atomic numbering.

All the results of the X-ray diffraction of **5** indicate the formation of a mononuclear osmocenium salt and no evidence for formation of biosmocene was found. However the result is very valuable for the metallocene chemistry.

The Os–Cp and Os–C_{ring} distances are 1.857(5) and 2.20(6) Å, respectively, the latter value is closer to those of osmocene[13] and $[Os^{II}Cp_2–Hg–Os^{II}Cp_2]^+$ cation,[7] however the formal oxidation state of Os is Os^{IV}. The most interesting structural feature of the cation is the coordination of the F atom of the BF_4^- ion to the Os^{IV} center to fulfill the 18-electron rule around the Os atom.

Table 4. Selected Bond Distances and Angles for **5**

Atom 1	Atom 2	Dist/Å	Atom 1	Atom 2	Dist/Å
Os(1)	C(1)	2.15 (1)	Os(1)	C(2)	2.20 (1)
Os(1)	C(3)	2.27 (1)	Os(1)	C(4)	2.25 (1)
Os(1)	C(5)	2.16 (1)	Os(1)	C(6)	2.11 (1)
Os(1)	C(7)	2.21 (1)	Os(1)	C(8)	2.27 (2)
Os(1)	C(9)	2.23 (1)	Os(1)	C(10)	2.15 (1)
Os(1)	F(1)	2.07 (1)			
C(1)	C(2)	1.40 (2)	C(1)	C(5)	1.33 (2)
C(2)	C(3)	1.33 (2)	C(3)	C(4)	1.48 (3)
C(4)	C(5)	1.37 (2)	C(6)	C(7)	1.26 (2)
C(6)	C(10)	1.28 (3)	C(7)	C(8)	1.30 (4)
C(8)	C(9)	1.68 (3)	C(9)	C(10)	1.38 (2)
B(1)	F(1)	1.51 (2)	B(1)	F(2)	1.37 (2)
B(1)	F(3)	1.40 (2)	B(1)	F(4)	1.36 (2)
B(2)	F(5)	1.33 (2)	B(2)	F(6)	1.27 (3)
B(2)	F(7)	1.30 (2)	B(2)	F(8)	1.23 (4)
Bond angles					
B(1)	F(1)	Os(1) 130.6(7)	Cp(1)	Os(1)	Cp(2) 140(3)

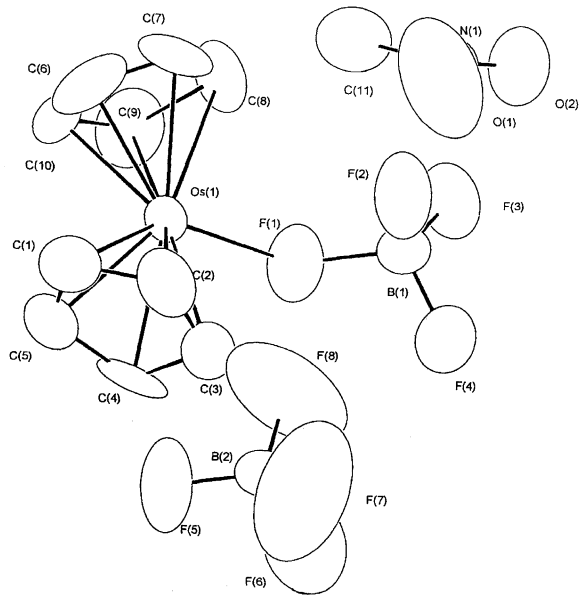

Fig. 3. ORTEP drawing of **5** with the thermal ellipsoids at the 50% probability level.

The F(1)–Os(1) distance is 2.07(1) Å (which is close to the sum of atomic radii (2.03 Å) of the fluorine (0.68 Å) and osmium (1.35 Å) atoms), indicating that the coordination of the F^- atom in the BF_4^- anion to the Os atom is verified and the cation is formulated as $[Cp_2Os^{IV}FBF_3]^+$. This is the first example of the coordination of the BF_4^- anion to the central metal atoms in metallocene chemistry to our knowledge. The F(1)···C(3), F(1)···C(4), and F(1)···C(8) distances were found to be 2.73(1), 2.94(2), and 2.74(2) Å, respectively, which are much smaller to the sum (3.05 Å) of the van der Waals radii of the C and the F atoms. The two Cp-planes in the osmocene moiety are highly slanted as in the case of halometallocenium cations $[MCp_2X]^+$ and Hg adducts of metallocenes.[14] The tilting angle between the planes C(1-5) and C(6-10) is 40(3)°, which is much larger than the values in $[OsCp_2–Hg–OsCp_2]$ (34.46° and 27.32°[14]) and $[Cp_2Os–OsCp_2]$ (35.5°[7]).

The F(1)–B(1) distance is 1.51(2) Å, which is much longer than the those of other B(1)–$F_{2,3,4}$ bonds (1.36—1.40 Å) and BF_4^- (1.23—1.33 Å). This must be due to the coordination of the F(1) atom to the Os^{IV} atom. The B(1)–F(1)–Os(1) bond angle is 130.6(7)°, this is closer to the value of B–F–B (129(1)°) of $B_2F_7^-$ in **3**.

It can be concluded that the oxidation of osmocene by the excess of *p*-Bq/BF_3 in benzene–hexane gives no dimerized salts like in the case of ruthenocene but gives the mononuclear cation, $[Cp_2Os^{IV}FBF_3]^+$. To investigate the mechanism of the formation of **5** (Scheme 3), the oxidation of osmocene with various amounts of *p*-Bq/BF_3 was pursued in detail by the ^{1}H NMR study in CD_3NO_2 (a poor donor solvent). The ^{1}H NMR spectrum of osmocene in CD_3NO_2 gave a sharp signal at δ = 4.73. To the solution, 0.5 equivalent of *p*-Bq/BF_3 is added. The color of the solution immediately changed to green, which is the color of the typical osmocenium salt containing Os^{III}. The solution gave a sharp signal at δ = 5.86, which corresponds well with that of the $[Cp_2Os–OsCp_2]^{2+}$ cation (**6**) (Ref. δ = 5.88[7]). Actually by adding NH_4PF_6 to the solution, well-formed green salt as the major products could be collected from the solution, the ^{1}H NMR spectrum of which corresponds with that of the reported salt $[Cp_2Os–OsCp_2](PF_6)_2$. Thus, osmocene was mono-oxidized by 0.5 equivalent of Bq/BF_3 to give the cation **6** containing the direct Os^{III}–Os^{III} bond which gives some stability to the osmocenium cation to fulfil the 18-electron rule. To the green solution, 0.5 equivalent of *p*-Bq/BF_3 was added, and then the color changed to yellow-orange, rapidly. The solution gave a signal at δ = 6.09, which agreed with the value for **5**, indicating that **6** is oxidized to **5**, which contains the Os^{IV}–F^- bond in CH_3NO_2. The driving force of the coordination of the F^- to the Os atom may be due to the greater softness of the Os atom in osmocene compared with the Ru in ruthenocene.

Considering these facts, osmocene undergoes two elec-

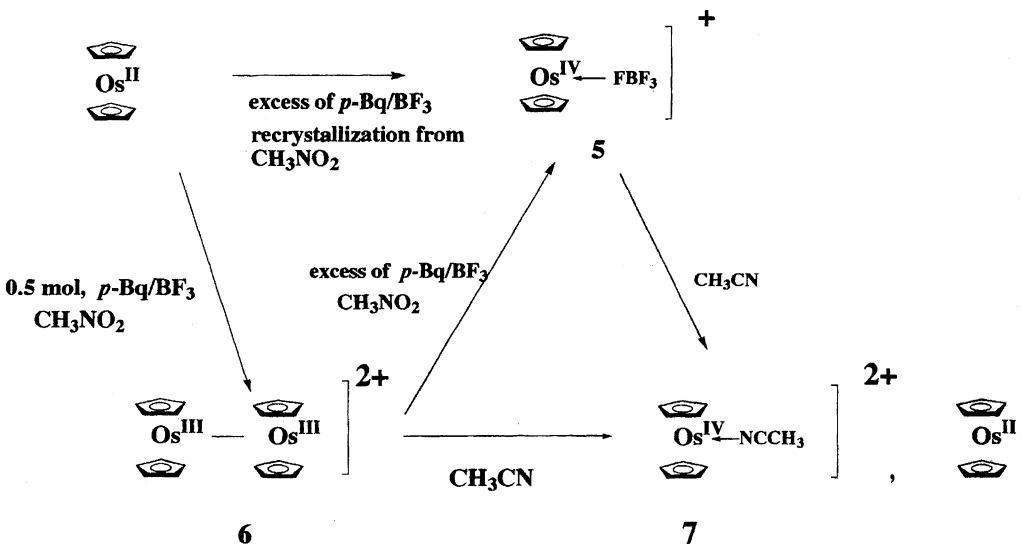

Scheme 3.

tron-oxidation by an excess of p-Bq/BF_3 in benzene–hexane directly giving insoluble dark-yellow precipitates. Recrystallization of the salt from CH_3NO_2 gave an orange-red salt, $[Cp_2Os^{IV}FBF_3](BF_4)CH_3NO_2$, **5** as a major product. The coordinated BF_4^- ion **5** is replaced by CH_3CN slowly and gives the reported salt **7**, based on the results of an ^1H NMR study in CD_3CN. The p-Bq/BF_3 oxidation of ferrocene gives a ferrocenium cation formulated as $[Cp_2Fe^{III}]^+$; this cation is very stable in many polar solvents. Therefore, it can be concluded that the great stability of the cations $[Cp_2M^{III}]^+$ (M = Fe, Os) prevent the coupling reactions observed for ruthenocenium dication. The instability of the $[Cp_2Ru^{III}]^+$ cation gives the hydrogen abstraction from another ruthenocene to give ruthenocenyl radicals in less nucleophilic solutions (C_6H_6, CH_2Cl_2, et al.), which couple with each other giving a dimer product. These chemical reaction may be one of the possible reasons for occurrence of the irreversible 2e-oxidation cyclic voltammograms for ruthenocene in normal supporting electrolyte, except for a noncoordinating supporting electrolyte (TBA^+TFPB^-) in CH_2Cl_2.[3] Figure 4 shows the multi scan (scan time n = 6) cyclic voltammetric behavior of ruthenocene in CH_2Cl_2 containing 0.1 M $(n\text{-Bu})_4NClO_4$ as supporting electrolyte.

As is well known, an irreversibility one-step 2e-oxidation wave is observed at about 0.48 V (**O_1**, first scan n = 1, in V vs. ferrocene-ferrocenium); the peak intensity is getting smaller and smaller and the second oxidation peak intensity (**O_2**, E_{pa} = about 0.17 V) is increasing for multi scan cyclic voltammograms (n = 2—6), and the E_p value for the latter peak corresponds with that of biruthenocene (E_{pa} = about 0.21 V) for the same conditions. This observation suggests that some species of unstable $[Cp_2Ru^{III}]^+$ cation as the first oxidation products of ruthenocene on the surface of the electrode give the protonated cation $[Cp_2Ru^{III}H]^+$ and the ruthenocenium radical (see Scheme 2) and the latter gives biruthenocenium dication on the electrode at this potential. The reduction of the dication gives biruthenocene through the backscan, therefore a new oxidation peak, **O_2**, is observed for multi scan waves. The intensities of **O_2** is much less than that of **O_1**, due to the loss of the biruthenocene by diffusion from the surface of the electrode. Absence of the same cyclic voltammetric behavior of ruthenocene was found in CH_3CN because the unstable $[Cp_2Ru^{III}]^+$ cations give the stable $[RcHNCCH_3]^+$ and $[RcHNCCH_3]^{2+}$ cations (ECE-mechanisms) at the surface of the electrode.[5]

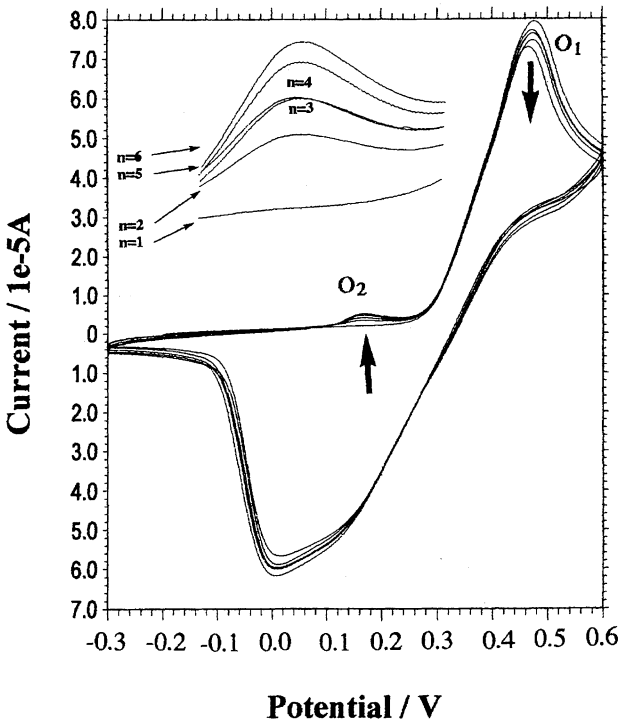

Fig. 4. Cyclic voltammogram of ruthenocene (1 mM) in CH_2Cl_2.

From the results of these studies, it can be concluded that the dimerization salt (**A**) was prepared by the oxidation of RcH in less polar solvents, this is the most elegant preparation of biruthenocene. Recrystallization of **A** containing RCN (R = CH_3, C_2H_5) or pyradine gave their mixed valence ($Ru^{II}Ru^{IV}$) salts (deep red precipitates) formulated

as $[Ru^{II}Cp(C_5H_4C_5H_4)CpRu^{IV}L]^{2+}$. On the other hand, recrystallization of **A** from less coordinated solvents such as CH_3NO_2 gave yellow-orange precipitates in which the formal oxidation states of the Ru atom in both ruthenocenyl moiety are equivalent from the ^1H NMR spectra. That is, four signals at δ = 5.79 (s) assigned to the Cp ligand and δ = 6.82 (t), 4.96 (t) to the $C_5H_4C_5H_4$ ligand were found and a surprisingly large chemical shift difference ($\Delta\delta$ = 1.86 ppm) is found for the $C_5H_4C_5H_4$ ligand, suggesting the large coordination mode change of the fulvalene ligand from that of biruthenocene and its reported mixed valence salts (**1**—**3**). The ^{13}C NMR spectrum of **A** in CD_3NO_2 shows four signals at δ = 89.7 assigned to the Cp ligand, δ = 95.7, 87.0 to the $C_5H_4C_5H_4$ ligand, and one weak signal at δ = 74.8 to the *ipso*-$C_5H_4C_5H_4$. A similar large $\Delta\delta$ (8.7 ppm) was observed for the fulvalene ligand ($\Delta\delta$ = 1.7 ppm for biruthenocene in $CDCl_3$[2]). Moreover, a quite large higher field shift of the *ipso*-carbon atom was found compared with that of neutral biruthenocene (δ = 87.5 in $CDCl_3$[2]), suggesting some interaction between Ru and *ipso*-carbon atoms. These results of NMR studies of **A** predict the formation of a novel structure Ru–fulvalene complex with a new coordination mode. To extend these chemistries, single X-ray analysis of **A** should be done.

References

1) M. Watanabe, I. Motoyama, T. Takayama, and M. Sato, *J. Organomet. Chem.*, **13**, 549 (1997).

2) M. Watanabe, T. Iwamoto, A. Kubo, S. Kawata, H. Sano, and I. Motoyama, *Inorg. Chem.*, **31**, 177 (1992).

3) M. G. Hill, W. M. Lamanna, and K. R. Mann, *Inorg. Chem.*, **30**, 4690 (1991).

4) L. Pauling, "The Nature of the Chemical Bond," 3 rd ed, Cornell Univ. Press (1960).

5) H. Ogino, H. Tobita, K. Hashidzum, and M. Shimoi, *J. Chem. Soc., Chem. Commun.*, **1989**, 828; K. Habazaki, H. Tobita, and H. Ogino, *Organometallics*, **14**, 1187 (1995).

6) K. Kirchner, K. Mereiter, R. Schmid, and H. Taube, *Inorg. Chem.*, **32**, 5553 (1993).

7) M. W. Droge, W. D. Hamman, and H. Taube, *Inorg. Chem.*, **26**, 1309 (1987).

8) D. P. Rillema, D. S. Jones, C. Woods, and H. A. Levy, *Inorg. Chem.*, **31**, 2935 (1992).

9) A. N. Nesmeyanov, L. S. Isaeva, and T. A. Peganova, *Dokl. Chem. (Engl, Transl.)*, **235**, 380 (1977); A. N. Nesmeyanov, L. S. Isaeva, and T. A. Peganova, P. V. Petrovskii, A. I. Lutsenko, and N. I. Vasyukova, *J. Organomet. Chem.*, **172**, 185 (1979).

10) M. D. Glick and L. F. Dahl, *J. Organomet. Chem.*, **3**, 200 (1965).

11) P. S. Maddren, A. Modinos, P. L. Timms, and P. Woodward, *J. Chem. Soc., Dolton Trans.*, **1975**, 1272; J. A. K. Howard, I. W. Kerr, and P. Woodward, *J. Chem. Soc., Dolton Trans.*, **1975**, 2466.

12) G. E. Heberich and B. Hessner, *J. Organomet. Chem.*, **161**, C36 (1978).

13) F. Z. Jellonek, *Z. Natureforsch., B*, **14B**, 737 (1959).

14) M. Watanabe, A. Nagasawa, M. Sato, I. Motoyama, and T. Takayama, *Bull. Chem. Soc. Jpn.*, **71**, 1071 (1998).